NASA Contractor Report 204145

Design and Fabrication of a Dielectric Total Internal Reflecting Solar Concentrator and Associated Flux Extractor for Extreme High Temperature (2500K) Applications

Jack A. Soules
Analex Corporation
Brook Park, Ohio

Donald R. Buchele
ADF Corporation
Brook Park, Ohio

Charles H. Castle and Robert P. Macosko
Analex Corporation
Brook Park, Ohio

Prepared under Contract NAS3–27600

National Aeronautics and
Space Administration

Lewis Research Center

November 1997

Available from

NASA Center for Aerospace Information
800 Elkridge Landing Road
Linthicum Heights, MD 21090-2934
Price Code: A03

National Technical Information Service
5287 Port Royal Road
Springfield, VA 22100
Price Code: A03

Design and fabrication of a dielectric total internal reflecting solar concentrator and associated flux extractor for extreme high temperature (2500K) applications

Jack A. Soules[a], Donald R. Buchele[b], Charles H. Castle[a], and Robert P. Macosko[a]

[a]Analex Corporation, 3001 Aerospace Parkway, Brook Park, Ohio 44142

[b]ADF Corporation, 3003 Aerospace Parkway, Brook Park, Ohio, 44142

ABSTRACT

The Analex Corporation, under contract to the NASA Lewis Research Center (LeRC), Cleveland, Ohio, recently evaluated the feasibility of utilizing refractive secondary concentrators for solar heat receivers operating at temperatures up to 2500K. The feasibility study pointed out a number of significant advantages provided by solid single crystal refractive devices over the more conventional hollow reflective compound parabolic concentrators (CPCs). In addition to the advantages of higher concentration ratio and efficiency, the refractive concentrator, when combined with a flux extractor rod, provides for flux tailoring within the heat receiver cavity. This is a highly desirable, almost mandatory, feature for solar thermal propulsion engine designs presently being considered for NASA and Air Force solar thermal applications.

Following the feasibility evaluation, the NASA-LeRC, NASA-Marshall Space Flight Center (MSFC), and Analex Corporation teamed to design, fabricate, and test a refractive secondary concentrator/flux extractor system for potential use in the NASA-MSFC "Shooting Star" flight experiment. This paper describes the advantages and technical challenges associated with the development of a refractive secondary concentrator/flux extractor system for this application. In addition it describes the design methodologies developed and utilized and the material and fabrication limitations encountered.

Keywords: solar power, solar thermal power, solar concentrators, secondary concentrators, nonimaging solar concentrators, dielectric solar concentrators, solar flux extractors, solar flux tailoring, high temperature coatings, high temperature optical crystals, high temperature thermal conductivity, thermal contact resistance

1. INTRODUCTION

Design operating temperatures for proposed solar thermal power and propulsion systems are at levels approaching 2500K. These high temperature systems have driven the requirement for the sun collection system to achieve solar concentration ratios (CR) in the 8000 to 10000:1 range. The CR is the ratio of the primary mirror solar collection area to the entrance aperture area in the solar heat receiver. The aperture area significantly affects the amount of infra-red (IR) radiation which escapes from the receiver cavity (reflux) at 2500K and it therefore must be minimized. Primary concentrators (rigid or inflatable) cannot focus to the accuracy required to achieve the high CR and therefore secondary non-imaging concentrators must be included in the system design.

A significant amount of research and development has already been accomplished on non-imaging hollow reflective compound parabolic concentrators (CPCs) (Ref. 1). Secondary concentrators utilizing solid high index of refraction materials take advantage of both refraction and loss-less total internal reflection (TIR) and have been identified as the best in achieving maximum CR and highest efficiency. (Ref. 2). Reference 2 also identifies a concentrator shape that differs from the standard parabolic shape and achieves high CR in a smaller and easier to fabricate package. This type of device has been named a dielectric total internal reflecting concentrator (DTIRC).

A feasibility study to evaluate the performance benefits of incorporating refractive secondary concentrators in the design of high temperature heat receivers was recently completed by Analex Corporation under contract to NASA

LeRC. The results of this study led to the decision by NASA-MSFC to fund the design, fabrication, and test of a DTIRC and flux extractor for potential use in their "Shooting Star " flight experiment to be flown in 1999. The flight experiment will demonstrate all the technologies associated with a solar thermal propulsion system (ie. primary concentrator with an inflatable support structure, secondary concentrator, pointing and tracking system, high temperature engine/thruster, etc.). The results of that study, the resulting design concept and analysis, and some preliminary materials considerations are presented herein.

2. DESIGN CONCEPT

The design concept for the "Shooting Star" engine with the proposed DTIRC and flux extractor is shown in Fig. 1. Solar energy from a Fresnel primary concentrator (not shown) enters the DTIRC at a 22 degree entrance half angle. The DTIRC is shaped such that rays crossing a sub wavelength gap between the DTIRC and flux extractor rod are limited to angles that maintain TIR in the flux extractor. The solar energy exits the extractor at three faceted surfaces. The sub wavelength gap (<1/20 wave) provides an efficient optical connection for passing solar energy from the DTIRC to the extractor. In addition it provides a thermal break between the hot extractor and the cooler DTIRC to reduce heat conduction losses. The DTIRC is held in contact with the extractor by spring force and both are fastened to the front mounting plate. The DTIRC and flux extractor are each fabricated from single crystal zirconium oxide (yttria stabilized) which has a melt point of about 3000K and an index of refraction of 2.16. Preliminary analysis indicates that, while the extractor will operate at the engine cavity temperature, the DTIRC will operate at temperatures below 1000K.

The engine is constructed of rhenium and is designed for use with hydrogen propellant at temperatures approaching 2500K. The flight experiment is to be placed in orbit by the Shuttle and, for safety reasons, nitrogen gas will be used instead of hydrogen. The nitrogen propellant enters the engine, flows through a rhenium foam filled annulus around the receiver cavity and, for this experiment, is heated to temperatures approaching 2000K, expanding through the nozzle producing a gain in specific impulse over cold gas.

The use of the DTIRC and flux extractor for the "Shooting Star" experiment offers the following significant advantages over a hollow reflective secondary concentrator:

- Provides higher throughput (efficiency)
- Requires no special cooling device
- Blocks heat receiver material boiloff from the cavity
- Provides for flux tailoring in the cavity via the extractor
- Provides potential reduction of IR reflux from cavity (IR block coating)

Additional information on the detailed design, material properties and availability, special coatings being considered, and fabrication challenges and limitations is presented in Sections 4 and 5.

3. ANALYSIS

The overall efficiency of a DTIRC and flux extractor used in applications typical of the "Shooting Star" engine concept is influenced by the following :

- Reflection loss at the DTIRC inlet spherical surface
- Energy absorbed in the DTIRC
- Energy back reflected by the DTIRC
- Energy back reflected at the sub wavelength gap
- Energy back reflected from the flux extractor
- IR reflux loss from the cavity
- Thermal conduction from the extractor to the DTIRC
- Energy back reflected due to DTIRC surface fabrication error and/or component alignment error.

The reflection loss at the DTIRC spherical inlet surface can be reduced to ~1% of the input power by the application of an anti reflective (AR) coating. This surface is expected to run relatively cool (below 1000K). AR coatings are commercially available that can survive at this temperature.

Single crystal materials being considered for the DTIRC (sapphire, zirconia, and magnesium oxide) are transparent to the solar spectrum at all wave lengths up to 5 or 6 microns. The assumption that all the available energy above 5 microns is absorbed in the DTIRC results in a negligible energy loss due to absorption (~0.5%).

Energy losses due to fabrication and/or component alignment errors are specific to each application and are not addressed in this paper.

Detailed analyses using Opticad, Zemax, and ANSYS computer software have been performed to evaluate the remaining potential losses. A summary of the results is presented in the following discussion.

3.1 Flux extractor efficiency determination_

During the initial ray tracing analyses of concentrator shapes it was learned that a significant amount of energy was back reflected from the DTIRC exiting surface due to Fresnel reflection and to TIR. It was estimated that over 50% of the available energy would be lost. Various DTIRC exiting surface shapes were evaluated with no significant improvement. Extension pieces of various shapes and lengths were then evaluated with improved results. Finally it was found that a dielectric rod (flux extractor), mechanically and optically attached to the exit of the DTIRC, provided the best performance. In addition the dielectric rod allowed for the tailored distribution of the solar flux which could be accomplished by either applying facets to the rod , by creating diffuse surfaces on the rod, or a combination of both.

An acrylic DTIRC and flux extractor were fabricated to demonstrate the optics (Fig. 2). The extractor in Fig. 2 is made of three facets on a rod, forming a pyramid as described in Ref. 3. The results of a typical 3D ray trace for the acrylic demonstrator are presented in Fig. 3. The extracted energy is uniformly distributed around the circumference, with an axial distribution as illustrated in the figure. The axial distribution shown is based on a uniform distribution of solar energy entering the DTIRC.

All the flux is not extracted if the pyramid length is too small or the refractive index too large. The Opticad analysis showed that some flux is reflected back to the DTIRC. The fraction reflected is plotted in Fig. 4 against refractive index for two pyramid cross-section shapes, an equilateral triangle similar to that in Reference 3, and a 45 degree isosceles triangle, with four ratios of pyramid length to diameter (L/D). At the index of silica or acrylic, both shapes have a small reflection at all L/D's. At the much greater index of zirconia, the 45 degree isosceles pyramid was found to be an optimum shape. At L/D=5, the change from equilateral to isosceles shape reduced the reflection from 14.5 to 6 percent. L/D=6 reduces the reflection from 12 to 3 percent. A four-sided 45/135 degree pyramid potentially has the same performance as the isosceles shape but is more symmetrical. The four-sided shape is presently being studied.

The flux extracted is a large fraction of all flux transmitted by the rod to the pyramid. Each ray extracted at the pyramid surface has been split into two rays by Fresnel reflection. A fraction of the ray energy is extracted. The remaining ray energy is reflected inside the tip to the next surface intersection for further extraction. Rays not extracted are reversed in a direction toward the DTIRC. In this direction the extraction also continues. Rays not extracted in the rod enter the DTIRC and are lost. This ray energy is the reflection loss shown in Fig. 4.

3.2 Solar flux loss by reflection from gap

The DTIRC transmits flux to the flux extractor at a high temperature inside the receiver. To optically join the two pieces and to reduce the conduction heat loss back to the DTIRC, a flat surface vacuum gap is used at the DTIRC exit in Fig. 1. A large gap causes a zirconia DTIRC exit surface to reflect 67% of the solar flux back through the DTIRC and out to the primary collector. This loss is caused mainly by TIR with an additional 13% from Fresnel reflection. As the gap is reduced to less than a wavelength the TIR is increasingly frustrated, so more flux is transmitted. The back-reflected flux is a sum over wavelength and angle of incidence on the gap surface. Polarization analysis was used to determine the fraction reflected. Shown in Fig. 6 are the resulting reflection losses plotted for sapphire and zirconia versus the gap dimension for several maximum ray exit angles from the DTIRC. The maximum ray angle that provides for TIR of all rays in the flux extractor is 56 degrees for sapphire, and 67 degrees for zirconia. At a ray angle of 67 degrees for zirconia, a gap 1/20th of a 0.5 micron wavelength or .025 microns, the reflection loss is 0.17 (17%). A

1/40th wavelength gap reduces the reflection factor to 5%. This small gap is still expected to be a thermal break that can reduce heat conducted to the DTIRC.

3.3 Infrared loss by radiation from receiver cavity

To estimate the flux radiated back from the receiver cavity, note that most of the flux follows two paths in reverse of the way it enters the cavity through the flux extractor. The main part from the receiver at temperature T_1 in Fig. 4 (inset) enters the extractor tip, goes through the rod at incidence angles greater than the rod TIR angle, then enters the DTIRC. Rays at less than the DTIRC maximum ray exit angle are focused to the primary collector. The second part from the receiver at temperature T_2 enters the rod near the DTIRC exit at rod internal incidence angles less than the TIR angle. Some of this flux is Fresnel reflected at the rod surface and remains in the receiver. The rest of the flux enters the rod and DTIRC and passes through the DTIRC with more than one reflection and exits from the front face. Some of this flux may be transmitted through the DTIRC side surface if TIR is frustrated. These two fluxes are transmitted through the rod at wavelengths shorter than an average cutoff wavelength λ_C. At longer wavelengths the dielectric is treated as a complete absorber. The third flux is emitted by the rod at a temperature T_3 and wavelengths greater than λ_C at the gap. Most of this flux is absorbed by the DTIRC.

The Opticad program was used to calculate the fraction of the entering rays which do not meet the TIR criterion on entering the extractor rod. This fraction is, of course, a function of the index of refraction of the material. The results are shown on the log-log graph of Fig. 6 where the fraction of nonreflected rays clearly follows a $1/n^{3.5}$ function. Since rays entering the rod from the receiver follow a similar path back out through the DTIRC, they can be counted using the same function which appears in Eq. 1, multiplying the loss term at T_2.

Similarly, rays returning from the receiver through the extractor tip and exiting back through the DTIRC can also be calculated. The resulting curve is labeled T_1 in Fig. 6 and leads to a $1/n^{3.25}$ factor in Eq. 1.

Thus the total flux passing through the dielectric rod of area A and index n is

$$\phi = \pi n^2 A[(1-1/n^{3.25}) \int_o^{\lambda c} L_\lambda (T_1) d\lambda + (1/n^{3.5}) \int_o^{\lambda c} L_\lambda (T_2) d\lambda + \int_{\lambda c}^{\infty} L_\lambda (T_3) d\lambda], \quad (1)$$

where $L_\lambda (T)$ is the receiver blackbody spectral radiance at temperature T. The two factors $1/n^X$ account for the skew ray solid angle subtended about area A. This solid angle is a fraction of π steradians. The factors were found using an optical analysis program with non-sequential ray tracing and a Lambertian ray-angle distribution. This solid angle is smaller than a meridian ray solid angle.

Equation (1) can be simplified if all three temperatures are taken to be equal, and the small difference of the factors $1/n^X$ is neglected. Then the flux loss is independent of the dielectric cutoff wavelength λ_C, giving

$$\phi = \pi n^2 A L(T), \quad (2)$$

where L is blackbody radiance. The product n^2A is a constant for a DTIRC with a given ray acceptance angle and inlet area. A change in index from air to any dielectric material changes area A but not the solar flux in or the IR flux loss. The IR flux loss is also independent of the DTIRC maximum ray exit angle with all three temperatures alike.

As an example of flux loss in a zirconia rod of index 2.16, area A cm^2, and T = 1500 K with L = 9.15 watts/(cm^2•steradian). The flux loss is ϕ /A = 132 watts/cm^2. At a temperature 2500 K, L = 70.6 watts/(cm^2•steradian), the flux loss is ϕ /A = 1019 watts/cm^2. These figures may be compared to the rod thermal conduction loss with and without a gap and to the solar flux loss at the gap.

3.4 Thermal analysis

Empirical data for the thermal and optical properties at high temperature of the single crystal materials being considered are very limited. Some are non-existent at the operating temperatures under consideration. Preliminary estimates of thermal performance were made by extrapolating data to the proposed operating conditions. A thermal and stress computer model is under development to assist in evaluating the performance at steady state and in transient mode. Detailed analysis of the radiation heat exchange between the DTIRC and the flux extractor is very complex

because the materials are both transparent and absorbent at various wavelengths. The computer model will attempt to bound the operating conditions using worst case assumptions and actual material property data where available.

It is expected that the sub wavelength gap will provide added resistance to heat conduction from the hot flux extractor to the cooler DTIRC. Tests are in process via a contract with Texas A&M University to measure the thermal contact resistance between highly polished single crystal materials in vacuum. Contact resistance data will be generated using polished zirconia and sapphire coupons for a range of contact pressures and temperatures. The results will be incorporated into the computer model as they become available.

4. MATERIALS SELECTION

4.1 Materials selection/characteristics

A number of optically clear single crystal materials are being considered for the DTIRC and the flux extractor ranging in index from 1.76 to 2.16. For the first test articles, the index of refraction was a secondary consideration with the primary concern being high melt point, manufacturing time, and availability in sufficient size. The known available materials are magnesium oxide (MgO), sapphire (Al_2O_3), and zirconia (ZrO_2). Thorium oxide (ThO_2) was also considered but was not available in sufficient size. Table 1 presents a comparison of the candidate materials. Useful data on these materials at temperatures above 2000K is sparse. Many of the entries in Table I are estimates.

Table I: Material Characteristics

Material	Size Availability	Melt Point	Index of Refraction	Est.Thermal Conductivity Watts/(cm•K)	Optical Absorption Cutoff	Chemical Stability
Al_2O_3 sapphire	13" dia x 6" long boules	~2300K	1.76	100 @ 20K .25 @ 300K .1 @ 1000K .06 @ 2300K	~5μ	Stable at high temp. in air or vacuum
MgO magnesium oxide	4" dia x 6" long irreg. shapes	~3000K	1.76	30 @ 20K .6 @ 300K .08 @ 1500K	~7μ	Reduces in air due to H_2O, stable at high temp. in vacuum
ZrO_2 zirconia	4" dia x 6" long irreg. shapes	~3000K	2.16	.1 @ 300K	~6μ	Reduces at high temp. in vacuum, stable in air

Yttria stabilized zirconia was selected as the material of choice for concept verification ground testing mainly due to its high melt point and lowest cost. The preferred material for the "Shooting Star" flight experiment has not yet been chosen.

5. DETAILED DESIGN, FABRICATION, AND TEST

5.1 Design methodology (DTIRC shape determination)

The DTIRC in Figure 1 is comprised of a spherical entrance surface and a conical side surface. A method has been developed to calculate a DTIRC geometry that provides TIR of all entering meridional rays, and also ensures TIR within the cylindrical portion of the flux extractor. This procedure is described in the next paragraph. To provide a foundation for the method a generic ray trace review is presented in Fig. 7. The extreme rays at the entrance half angle from the primary optics are used to define the geometry (Ref. 5). They enter at points A and C and, if the conical surface were not there, would converge at FP1 after refraction. When the conical surface is introduced, the extreme

rays refract and reflect by TIR to FP2 (the ray paths are mirror images about line CB). When the cylindrical flux extractor is introduced, the extreme rays reflect by TIR to FP3 (the ray paths are mirror images about line DE).

The DTIRC geometry is defined as follows, using Figs. 8 and 9. Fig. 8 shows the extreme left ray path as it enters at point A, refracts to point B and reflects in the flux extractor so that the incidence angle, alpha, is equal to the TIR angle for the crystal material being used. Fig. 9 shows the extreme right ray path as it enters at point C, refracts and reflects to point D, and reflects in the flux extractor so that the angle of incidence is again alpha.

To optimize the optical surfaces for this application begin by substituting several values of R, the radius of the spherical surface, in the equations for W1 and W3 as shown in Figs. 8 and 9. Plot W1 versus R and W3 versus R. The intersect point of the two curves determines the value of R where W1 = W3, and the exit diameter d2 = d1 - 2W1. The extreme rays in Figs. 8 and 9 are in the plane which contains the spherical and conical surface centerlines. They are meridional rays, and all such rays entering the DTIRC that are equal to or less than the entrance half angle, will internally reflect through the DTIRC and the flux extractor. The above calculations are first checked graphically by Computer Aided Design software (CAD). An Opticad ray trace analysis is then used to evaluate skew rays that enter the DTIRC. No rays are lost by back reflection in the DTIRC.

5.2 Manufacturing compromises

The DTIRC shape (a cone with a spherical inlet) is not necessarily the most efficient design for the refractive secondary but is the easiest to manufacture and is the smallest in physical size. A parabolic shape with a flat inlet surface maximizes the concentration ratio but is substantially longer. The increased size and the manufacturing difficulty in machining and polishing the parabolic surface create a much greater penalty than the gains due to a slightly higher concentration ratio.

The current apparent availability of materials and machining capability has limited the flux extractor size to a maximum length of ~6 inches for all of the materials being considered. The DTIRC size is similarly limited to ~4 inch inlet diameter and ~6 inch length.

5.3 Coatings development

Specialized coatings are being considered for thermal control and improved DTIRC and extractor efficiency. The following coatings are presently being developed and evaluated for potential use:

- Antireflective (AR) coating on the DTIRC spherical inlet face for improved efficiency
- Emissive coating on the DTIRC conical sides for thermal control
- IR block coating at the interface between the flux extractor and DTIRC for improved efficiency
- Low index coating for adjusting the TIR angle in the flux extractor for improved efficiency
- Low index coating for allowing attachment of hardware (maintains crystal TIR)

The DTIRC temperature is not expected to exceed 1000K at the inlet surface. AR coatings are commercially available that can operate at temperatures approaching 1000K. AR coatings for temperatures above 1000K require development. All of the other coatings listed above are for temperatures that will greatly exceed 1000K and the flux extractor temperature will approach maximum cavity temperatures of 2000K to 2500K. The development of these coatings is a significant challenge, but the reward in improved efficiency is also very significant.

5.4 Component testing

Coupons of zirconia, sapphire, and magnesium oxide with standard polished surfaces have been or are in the process of being prepared for various tests to determine compatibility with typical engine materials at the expected operating temperatures and in the space environment. These coupons are also being used to develop and evaluate the various coatings described above. In addition, coupons of zirconia and sapphire are being polished to 1/20 wave flatness (or best effort) for gap optical performance and thermal contact resistance determination.

Two full scale concentrator/extractor zirconia crystal sets are also being fabricated for optical and thermal performance testing in separate programs at the Marshall Space Flight Center. The crystal sets are designed for different power

levels and light entrance half angles and will be initially tested without coating enhancement except for the use of an anti reflective coating on the DTIRC inlet spherical surface.

All component testing is expected to be completed by late Fall, 1997, and the final design and material/coating choices for the Shooting Star Flight experiment finalized shortly after.

6. CONCLUDING REMARKS

At the present time the optical analysis and graphical design methods are well understood for sizing, shaping, performing efficiency trades, etc. on refractive secondary concentrators. By the end of 1997 the manufacturing and operating limitations or constraints should be well defined and goals for future development identified.

The refractive secondary concentrator is a viable alternative to reflective secondary concentrators for many solar thermal applications. The refractive secondary provides the significant advantages of flux tailoring, higher efficiency, and ease of cooling over the more conventional reflective types. In addition it provides for potential receiver cavity IR reflux reduction through the development of an IR block coating that can survive the high cavity temperature. Zirconia, magnesium oxide, and sapphire are candidate materials for the highest temperature applications but more work is needed to define the performance and operating limitations of these materials at the extreme temperatures desired for solar thermal propulsion. It is anticipated that NASA funding will continue to support the research and development of refractive secondary concentrators toward these goals.

ACKNOWLEDGMENTS

This work was supported by the National Aeronautics and Space Administration (NASA), Lewis Research Center under Contract NAS3-27600 (ARADS Task 0059).

The authors acknowledge the technical support provided by Michael Mirtich of the Analex Corporation in the area of specialized coatings for this application.

REFERENCES

1. SPIE Milestone Series Volume MS 106, *Selected Papers on Nonimaging Optics*, Roland Winston, Editor, 1995.

2. Xiaohui Ning, Roland Winston, and Joseph O'Gallagher, "Dielectric totally internally reflecting concentrators", *Applied Optics*, Volume 26(2), pp. 300-305. (January 15, 1987), 1987 Optical Society of America.

3. D. Jenkins, R. Winston, J. Bliss, J. O'Gallagher, A. Lewandowski, C. Bingham, "Solar Concentration of 50,000 achieved with output power approaching 1 kW" *Journal of Solar Energy Engineering*, Vol. 118, pp. 141-145, August, 1996.

4. H. Ries, A. Segal, and J. Karni, "Extracting concentrated light guide", *Applied Optics*, Volume 36, No. 13, pp. 2869-2874, May 1997.

5. M. Collares-Pereira, A. Rabl, and R. Winston, "Lens-mirror combinations with maximal concentration", *Applied Optics*, Volume 16, No.10, pp. 2677-2683, October 1977.

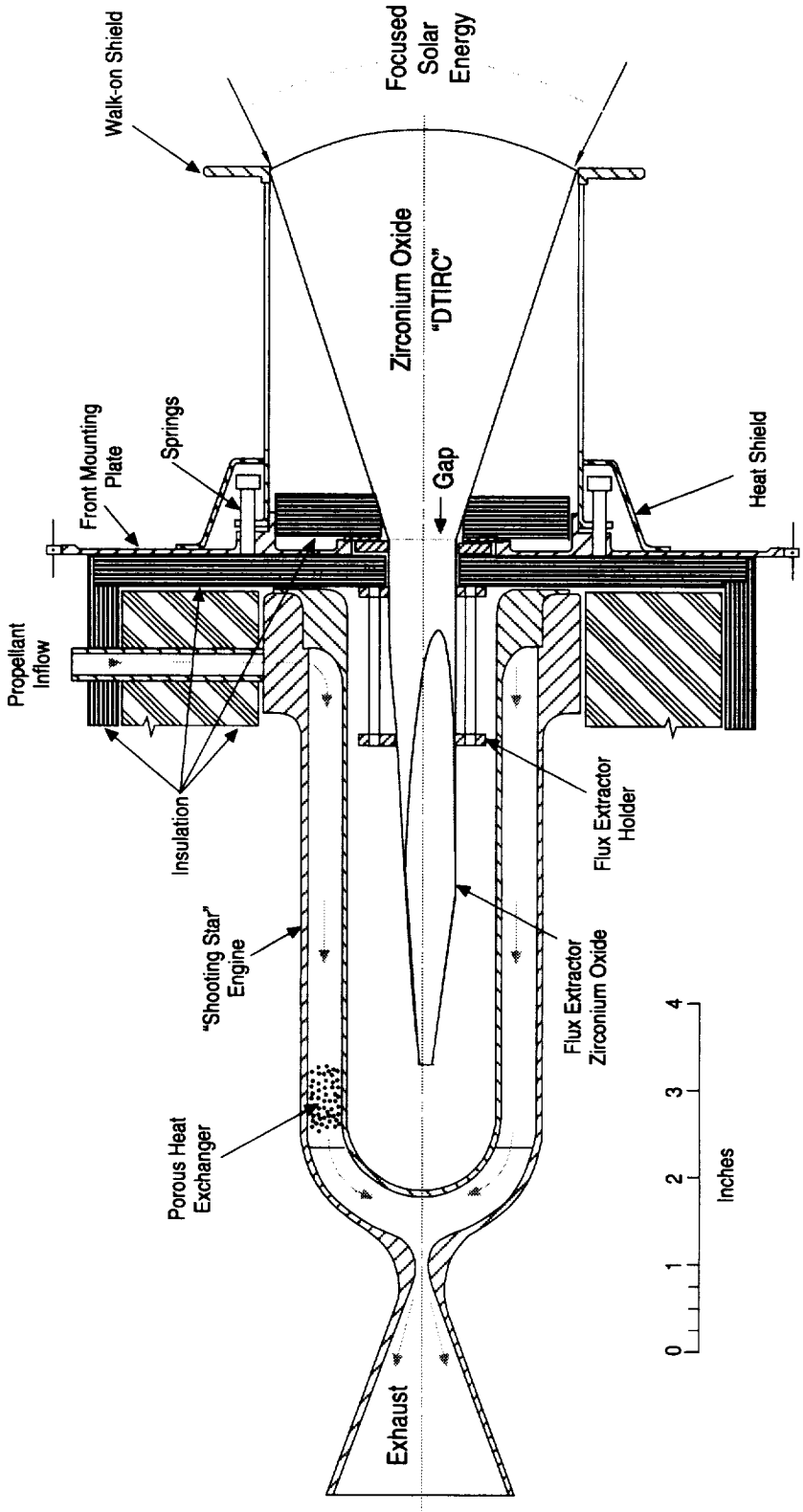

Figure 1. "Shooting Star" Engine Concept

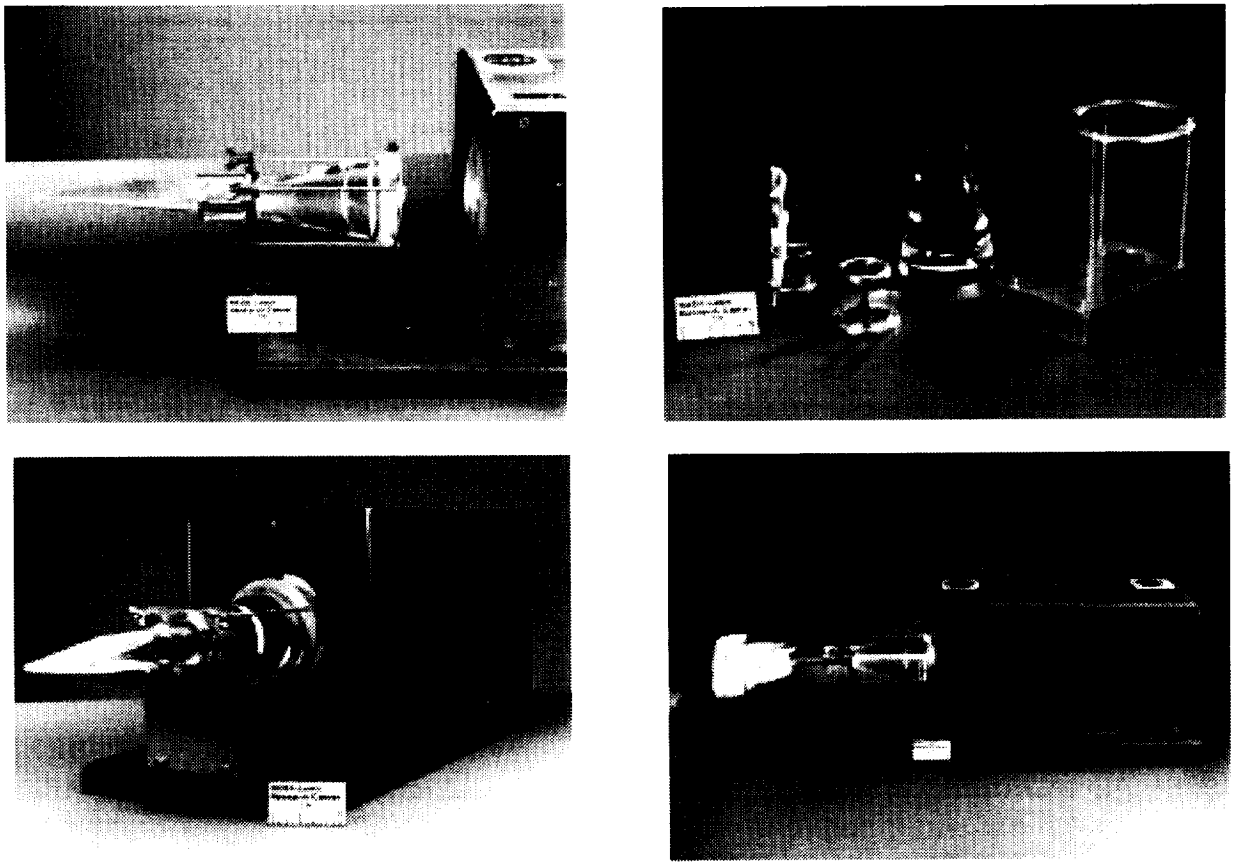

Figure 2. Acrylic Model (DTIRC and Extractor)

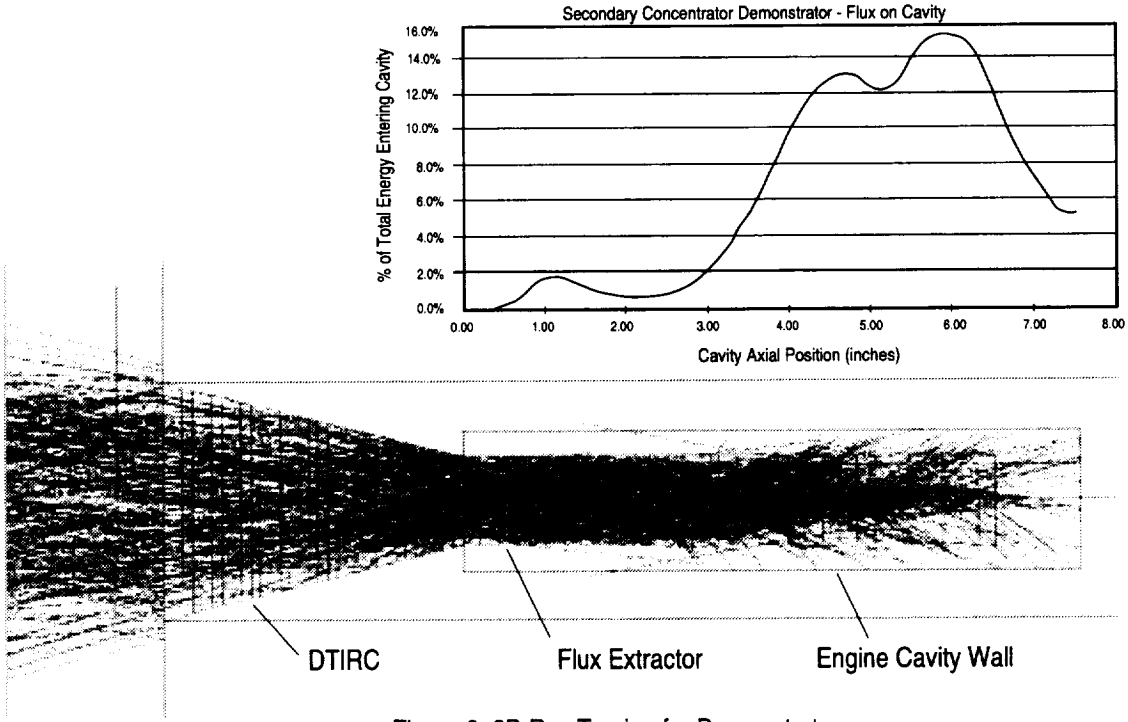

Figure 3. 3D Ray Tracing for Demonstrator

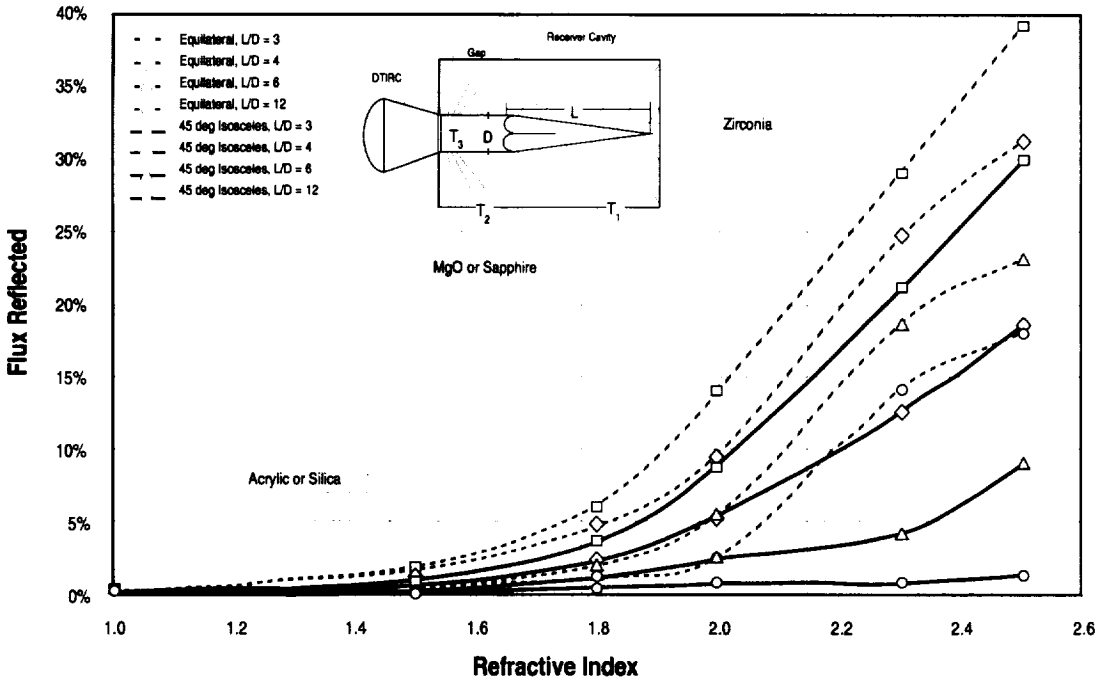

Figure 4. Reflection vs Refractive Index for Two Pyramidal Flux Extractors

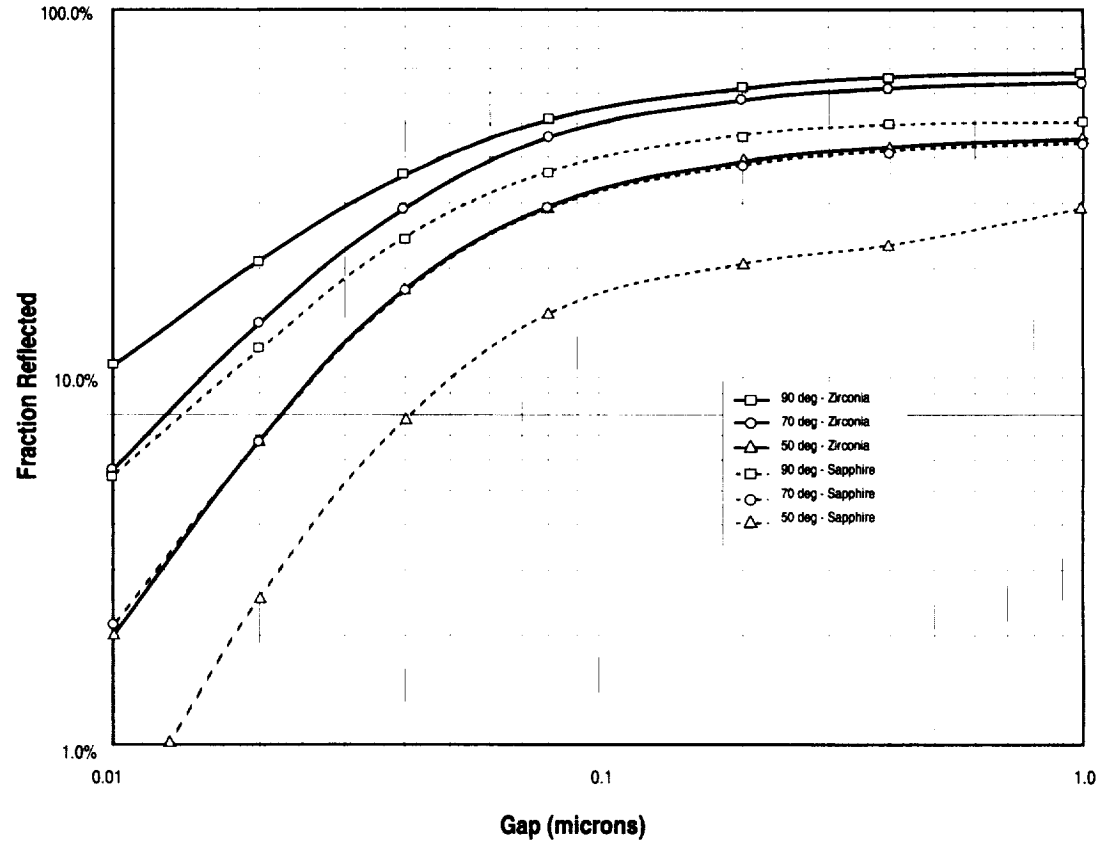

Figure 5. Reflection vs Gap at Three DTIRC Maximum Ray Exit Angles

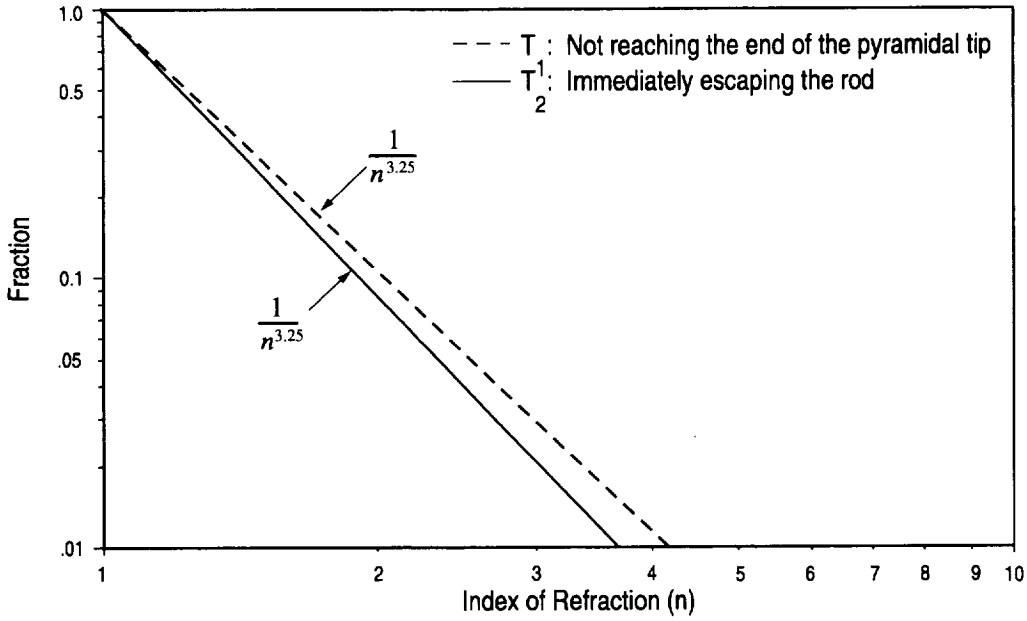

Figure 6. Fraction of Flux Leaving the Extractor Rod

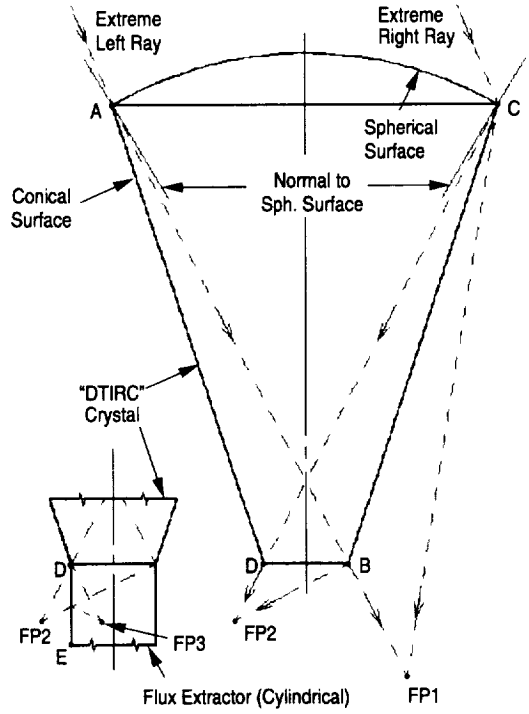

Figure 7. Generic Ray Trace Diagram

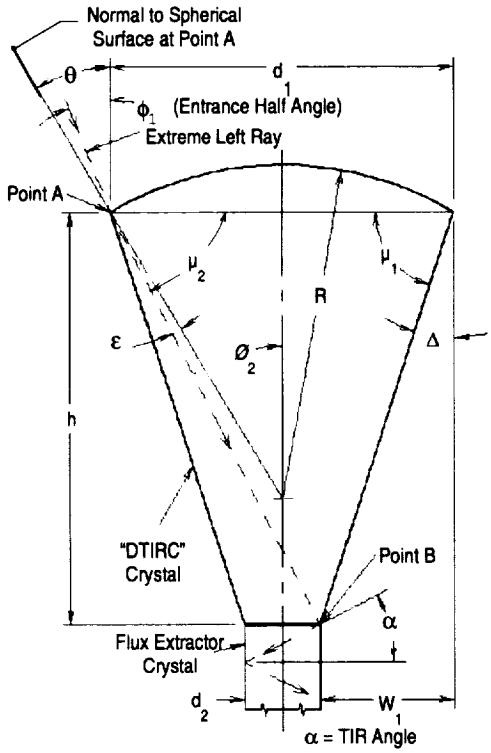

$$W_1 = d_1 - 2\left\{\left[d_1\frac{(\sin\mu_1)(\sin\mu_2)}{\sin(\mu_1+\mu_2)}\right]\left[\tan\frac{90-\alpha-\phi_2}{2}\right]\right\}$$

Figure 8. Extreme Left Ray Path

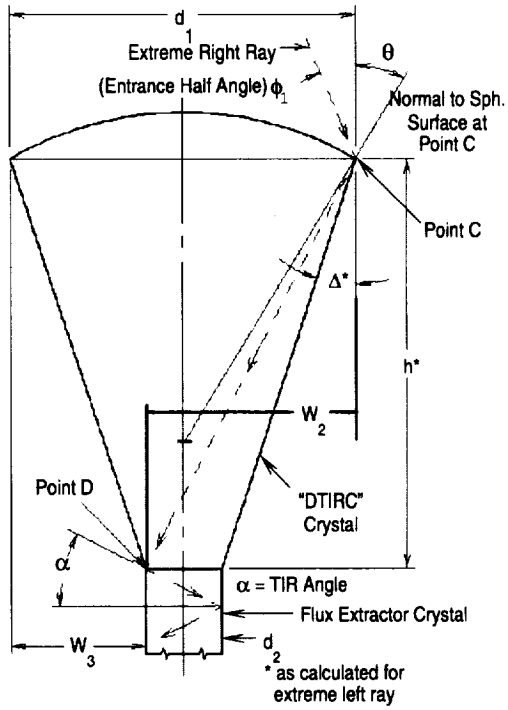

$$W_3 = d - h\tan\left\{\arcsin\left[\frac{\sin(\phi_1+\theta)}{n}\right] - \theta + 2\Delta\right\}$$

Figure 9. Extreme Right Ray Path

Key

$\theta = \arcsin\left(\frac{d_1}{2R}\right)$	$\varepsilon = \arcsin\left[\frac{\sin(\phi_1-\theta)}{n}\right]$ ε can be negative	n = Index of refraction of Crystal	$\phi_2 = \theta + \varepsilon$
$\Delta = \frac{90-\alpha-\phi_2}{2}$	$a = \arcsin\left(\frac{1}{n}\right)$	$\mu_1 = 90 - \Delta$	$\mu_2 = 90 - \phi_2$
$h = d_1\frac{(\sin\mu_1)(\sin\mu_2)}{\sin(\mu_1+\mu_2)}$	$W_1 = h\tan\Delta$ (See Fig. 8)	$W_3 = d_1 - W_2$ (See Fig. 9)	

REPORT DOCUMENTATION PAGE

Form Approved
OMB No. 0704-0188

1. AGENCY USE ONLY (*Leave blank*)	2. REPORT DATE	3. REPORT TYPE AND DATES COVERED
	November 1997	Final Contractor Report

4. TITLE AND SUBTITLE

Design and Fabrication of a Dielectric Total Internal Reflecting Solar Concentrator and Associated Flux Extractor for Extreme High Temperature (2500K) Applications

5. FUNDING NUMBERS

WU–953–73–10
C–NAS3–27600

6. AUTHOR(S)

Jack A. Soules, Donald R. Buchele, Charles H. Castle and Robert P. Macosko

7. PERFORMING ORGANIZATION NAME(S) AND ADDRESS(ES)

Analex Corporation
3001 Aerospace Parkway
Brook Park, Ohio 44142

8. PERFORMING ORGANIZATION REPORT NUMBER

E–10893

9. SPONSORING/MONITORING AGENCY NAME(S) AND ADDRESS(ES)

National Aeronautics and Space Administration
Lewis Research Center
Cleveland, Ohio 44135–3191

10. SPONSORING/MONITORING AGENCY REPORT NUMBER

NASA CR–204145

11. SUPPLEMENTARY NOTES

Jack A. Soules, Charles H. Castle, and Robert P. Macosko, Analex Corporation, 3001 Aerospace Parkway, Brook Park, Ohio 44142; Donald R. Buchele, ADF Corporation, 3003 Aerospace Parkway, Brook Park, Ohio 44142. Project Manager, Carol M. Tolbert, Power and On-Board Propulsion Technology Division, NASA Lewis Research Center, organization code 5490, (216) 433–6167.

12a. DISTRIBUTION/AVAILABILITY STATEMENT

Unclassified - Unlimited
Subject Category: 74 Distribution: Nonstandard

This publication is available from the NASA Center for AeroSpace Information, (301) 621–0390.

12b. DISTRIBUTION CODE

13. ABSTRACT (***Maximum 200 words***)

The Analex Corporation, under contract to the NASA Lewis Research Center (LeRC), Cleveland, Ohio, recently evaluated the feasibility of utilizing refractive secondary concentrators for solar heat receivers operating at temperatures up to 2500K. The feasibility study pointed out a number of significant advantages provided by solid single crystal refractive devices over the more conventional hollow reflective compound parabolic concentrators (CPCs). In addition to the advantages of higher concentration ratio and efficiency, the refractive concentrator, when combined with a flux extractor rod, provides for flux tailoring within the heat receiver cavity. This is a highly desirable, almost mandatory, feature for solar thermal propulsion engine designs presently being considered for NASA and Air Force solar thermal applications. Following the feasibility evaluation, the NASA-LeRC, NASA-Marshall Space Flight Center (MSFC), and Analex Corporation teamed to design, fabricate, and test a refractive secondary concentrator/flux extractor system for potential use in the NASA-MSFC "Shooting Star" flight experiment. This paper describes the advantages and technical challenges associated with the development of a refractive secondary concentrator/flux extractor system for this application. In addition it describes the design methodologies developed and utilized and the material and fabrication limitations encountered.

14. SUBJECT TERMS

Solar power; Solar thermal power; Solar concentrators; Secondary concentrators; Solar flux tailoring; High temperature crystals

15. NUMBER OF PAGES

18

16. PRICE CODE

A03

17. SECURITY CLASSIFICATION OF REPORT	18. SECURITY CLASSIFICATION OF THIS PAGE	19. SECURITY CLASSIFICATION OF ABSTRACT	20. LIMITATION OF ABSTRACT
Unclassified	Unclassified	Unclassified	